

Properties of the negative effective magnetic pressure instability

K. Kemel^{1,2,*}, A. Brandenburg^{1,2}, N. Kleeorin^{3,1}, and I. Rogachevskii^{3,1}

¹ Nordita**, AlbaNova University Center, Roslagstullsbacken 23, SE 10691 Stockholm, Sweden

² Department of Astronomy, AlbaNova University Center, Stockholm University, SE 10691 Stockholm, Sweden

³ Department of Mechanical Engineering, The Ben-Gurion University of the Negev, POB 653, Beer-Sheva 84105, Israel

Received 2011 Jul 14, accepted 2011 Nov 28

Published online 2012 Feb 15

Key words magnetohydrodynamics (MHD) – instabilities – turbulence

As was demonstrated in earlier studies, turbulence can result in a negative contribution to the effective mean magnetic pressure, which, in turn, can cause a large-scale instability. In this study, hydromagnetic mean-field modelling is performed for an isothermally stratified layer in the presence of a horizontal magnetic field. The negative effective magnetic pressure instability (NEMPI) is comprehensively investigated. It is shown that, if the effect of turbulence on the mean magnetic tension force vanishes, which is consistent with results from direct numerical simulations of forced turbulence, the fastest growing eigenmodes of NEMPI are two-dimensional. The growth rate is found to depend on a parameter β_* characterizing the turbulent contribution of the effective mean magnetic pressure for moderately strong mean magnetic fields. A fit formula is proposed that gives the growth rate as a function of turbulent kinematic viscosity, turbulent magnetic diffusivity, the density scale height, and the parameter β_* . The strength of the imposed magnetic field does not explicitly enter provided the location of the vertical boundaries are chosen such that the maximum of the eigenmode of NEMPI fits into the domain. The formation of sunspots and solar active regions is discussed as possible applications of NEMPI.

© 2012 WILEY-VCH Verlag GmbH & Co. KGaA, Weinheim

1 Introduction

The concept of turbulent viscosity is often used in astrophysical and other applications in recognition of the fact that the microscopic viscosity is far too small to be relevant on the length scales under consideration. Turbulent viscosity is the simplest parameterization of the Reynolds stress tensor, $\overline{u_i u_j}$, where $\mathbf{u} = \mathbf{U} - \overline{\mathbf{U}}$ is the velocity fluctuation about a suitably defined average, denoted here by an overbar. Turbulent viscosity is by far not the only contribution to the Reynolds stress tensor. In addition to hydrodynamic contributions such as the Λ effect (Rüdiger 1980, 1989), which is relevant to explaining stellar differential rotation (Rüdiger & Hollerbach 2004), and the anisotropic kinetic alpha effect (Frisch et al. 1987), which provides an important test case in mean-field hydrodynamics (Brandenburg & von Rekowski 2001; Courvoisier et al. 2010), there are magnetic contributions as well. One can think of them as a magnetic feedback on the hydrodynamic stress tensor (Rädler 1974; Rüdiger 1974) or, especially when magnetic fluctuations are also considered, as a mean-field contribution to the turbulent Lorentz force.

Work by Roberts & Soward (1975) and Rüdiger et al. (1986, 2012) using a quasi-linear approach suggests that the total magnetic tension force (which includes the effects of fluctuations) is reduced in the presence of a mean magnetic field and might formally even change sign for larger

magnetic Reynolds numbers, but this would then be beyond the validity of their approximation. Using the spectral τ approach, Kleeorin et al. (1989, 1990) do indeed find this reversal of the sign of the total magnetic tension force. In addition, they find a reversal of the sign of the effective magnetic pressure term; see also Kleeorin & Rogachevskii (1994) and Kleeorin et al. (1993, 1996). Rogachevskii & Kleeorin (2007) argue that, in a stratified medium, this can lead to the formation of large-scale magnetic flux structures and perhaps even sunspots – or at least active regions.

Recently, direct numerical simulations (DNS) of both unstratified and stratified forced turbulence (Brandenburg et al. 2010, 2012; hereafter referred to as BKR and BKKR, respectively) have substantiated this idea and have demonstrated that the effective magnetic pressure can indeed change sign. Similar results have now also been obtained for turbulent convection (Käpylä et al. 2012). In addition, these papers give results of mean-field calculations illustrating that there is a negative effective magnetic pressure instability (hereafter referred to as NEMPI) when there is sufficient density stratification.

NEMPI is a convective type instability related to the interchange instability in plasmas (Tserkovnikov 1960; Newcomb 1961; Priest 1982) and the magnetic buoyancy instability in the astrophysical context (Parker 1966). The free energy in interchange and magnetic buoyancy instabilities is drawn from the gravitational field, while in NEMPI it is provided by the small-scale turbulence.

The mechanism of NEMPI works even under isothermal conditions when entropy evolution is ignored and an

* Corresponding author: koentjekemel@hotmail.com

** Nordita is a Nordic research institute jointly operated by the Stockholm University and the Royal Institute of Technology, Stockholm.

isothermal equation of state is used. This has been shown using corresponding mean-field calculations (BKRR). With this reduction to the most elementary aspects of the instability, it has recently been possible to verify the existence of NEMPI also in DNS (Brandenburg et al. 2011, hereafter referred to as BKKMR). This has been a major step forward, because now there is no doubt that one is pursuing a real effect and not just one that works only in the world of mean-field models. Essential to the paper of BKKMR has been a finding from an earlier version of the present one that only two-dimensional mean-field structures are excited. This property allowed meaningful averaging along the direction of the imposed field, making the identification of flux concentrations thus much clearer. The absence of three-dimensional mean-field structures was surprising because three-dimensional mean-field calculations have shown that the mean magnetic field develops structures along the direction of the imposed field (BKR). However, while the mean-field calculations have illustrated the nature of the instability, no systematic survey of solutions has yet been attempted. The purpose of this paper is therefore to clarify some still puzzling aspects concerning NEMPI. Note also that the large-scale flux concentrations observed in DNS of BKKMR have an amplitude of only 15% of the local equipartition field. This implies that the flux concentrations we observe in DNS are often not strong enough to be noticeable without averaging.

In addition to the structures found in BKKMR, other types of structures have recently been reported in Large-Eddy Simulations (LES), which might also be an indication of NEMPI. We have here in mind the radiation magneto-convection simulations of Kitiashvili et al. (2010), in which one sees the formation of whirlpool-like magnetic structures. Relevant to NEMPI is also the work of Tao et al. (1998), who considered magneto-convection in the optically thick approximation and find a horizontal segregation into magnetized and non-magnetized regions. The size of the individual regions is such that they encompass several turbulent eddies. This phenomenon might therefore well be associated with an effect that could also be modelled in terms of mean-field theory. However, before we can make such an association, we need to find out more about the properties of NEMPI. In particular, we need to know what is the optimal magnetic field strength, what are the requirements or restrictions on the turbulent velocity, and, finally, how much density stratification is needed to make NEMPI work.

To connect the aforementioned requirements to DNS, we need to have a meaningful parameterization of the turbulence effects. The work done so far has been focussing on measuring a reduction of the turbulent pressure and effective mean magnetic pressure as a function of the local mean magnetic field strength. The shape of the resulting dependence of the effective mean magnetic pressure on the mean magnetic field has been matched to a specific fit formula that can be characterized by two fit parameters that, in turn, can be linked to the minimum effective mean magnetic

pressure and critical field strength above which the effect is suppressed. However, there have been indications that this parameterization is not unique and that different combinations of the two fit parameters can result in similar values of minimum effective pressure and the critical field strength. The question therefore arises whether this apparent degeneracy affects the properties of NEMPI.

We mentioned already the fact that NEMPI is capable of exciting three-dimensional structures that show variation along the direction of the mean magnetic field. This would give rise to the worry that the two-dimensional results presented so far may not reflect the properties of the fastest growing mode and may therefore not be relevant to describing NEMPI. However, as will be discussed in this paper, this is not the case, because the degree to which three-dimensional modes are excited depends on the sign and magnitude of one of the turbulence parameters, namely the term characterizing turbulence effects on the magnetic tension force, and that simulations indicate that this sign is not favorable for exciting three-dimensional modes (BKRR, Käpylä et al. 2012). Before we begin addressing the various points, we discuss first the mean-field model and basic setup.

2 Mean-field model

In view of further verifications of NEMPI with DNS, it is necessary to be able to reduce the essential physics to a minimum. We will therefore not make any attempt to consider other aspects that would make the model more realistic with respect to the Sun. Given that NEMPI works even under isothermal conditions (BKRR), we adopt an isothermal equation of state where the mean pressure \bar{p} is linear in the mean density $\bar{\rho}$, with $\bar{p} = \bar{\rho}c_s^2$ and c_s being the constant isothermal sound speed. We solve the evolution equations for mean velocity $\bar{\mathbf{U}}$, mean density $\bar{\rho}$, and mean vector potential $\bar{\mathbf{A}}$, in the form

$$\frac{\partial \bar{\mathbf{U}}}{\partial t} = -\bar{\mathbf{U}} \cdot \nabla \bar{\mathbf{U}} - c_s^2 \nabla \ln \bar{\rho} + \mathbf{g} + \bar{\mathcal{F}}_M + \bar{\mathcal{F}}_K, \quad (1)$$

$$\frac{\partial \bar{\rho}}{\partial t} = -\bar{\mathbf{U}} \cdot \nabla \bar{\rho} - \bar{\rho} \nabla \cdot \bar{\mathbf{U}}, \quad (2)$$

$$\frac{\partial \bar{\mathbf{A}}}{\partial t} = \bar{\mathbf{U}} \times \bar{\mathbf{B}} - (\eta_t + \eta) \bar{\mathbf{J}}, \quad (3)$$

where $\bar{\mathcal{F}}_M$ is given by

$$\bar{\rho} \bar{\mathcal{F}}_M = -\frac{1}{2} \nabla [(1 - q_p) \bar{\mathbf{B}}^2] + \bar{\mathbf{B}} \cdot \nabla [(1 - q_s) \bar{\mathbf{B}}], \quad (4)$$

and

$$\bar{\mathcal{F}}_K = (\nu_t + \nu) (\nabla^2 \bar{\mathbf{U}} + \frac{1}{3} \nabla \nabla \cdot \bar{\mathbf{U}} + 2 \bar{\mathbf{S}} \nabla \ln \bar{\rho}) \quad (5)$$

is the total (turbulent plus microscopic) viscous force. Here, $S_{ij} = \frac{1}{2} (\bar{U}_{i,j} + \bar{U}_{j,i}) - \frac{1}{3} \delta_{ij} \nabla \cdot \bar{\mathbf{U}}$ is the traceless rate of strain tensor of the mean flow. As in earlier work (BKR, BKKR), we approximate q_p and q_s by simple profiles that are only functions of the ratio $\beta \equiv |\bar{\mathbf{B}}|/B_{\text{eq}}$. However, in the earlier work this functional form was described by

$$q_\sigma(\beta) = q_{\sigma 0} [1 - (2/\pi) \arctan(\beta^2/\beta_\sigma^2)], \quad (6)$$

where B_{eq} is the equipartition field strengths and σ stands for subscripts p and s, respectively. We refer to this as the arctan fit. In the present paper we use an algebraic fit of the form

$$q_{\sigma}(\beta) = q_{\sigma 0} [1 - (2/\pi) \arctan(\beta^2/\beta_{\sigma}^2)], \quad (7)$$

$$q_{\sigma}(\beta) = \frac{q_{\sigma 0}}{1 + \beta^2/\beta_{\sigma}^2}. \quad (8)$$

The functions q_p and q_s quantify the impact of the mean magnetic field on the effective pressure and tension forces, respectively.

As initial condition, we assume a hydrostatic stratification with $\bar{\rho}(z) = \rho_0 \exp(-z/H_{\rho})$, where $H_{\rho} = c_s^2/g$ is the scale height in our domain of size $L_x \times L_y \times L_z$; the exact dimensions vary between 4 and 10 density scale heights in each direction. We add a small perturbation to the velocity field. We allow for the presence of an imposed field in the y direction, $\mathbf{B}_0 = (0, B_0, 0)$. The total field is then written as

$$\bar{\mathbf{B}} = \mathbf{B}_0 + \nabla \times \bar{\mathbf{A}}, \quad (9)$$

so the departure from the imposed field is expressed in terms of the mean magnetic vector potential $\bar{\mathbf{A}}$. Furthermore, we assume

$$B_{\text{eq}}(z) = B_{\text{eq}0} \exp(-z/2H_{\rho}), \quad (10)$$

with a normalization coefficient $B_{\text{eq}0}$. This formula is compatible with $B_{\text{eq}} = \rho^{1/2} u_{\text{rms}}$ in BKKMR, where the turbulent rms velocity, u_{rms} , was approximately constant.

On the upper and lower boundaries we adopt stress-free boundary conditions for velocity, i.e. $\bar{U}_{x,z} = \bar{U}_{y,z} = \bar{U}_z = 0$, and a perfect conductor boundary condition for the magnetic field, i.e. $\bar{A}_x = \bar{A}_y = \bar{A}_{z,z} = 0$. Here, commas denote partial differentiation. No boundary condition for the density is required. All computations have been carried out with the PENCIL CODE¹.

Our model is characterized by the following set of input parameters. There are three parameters characterizing the hydrostatic equilibrium stratification, namely g , c_s and ρ_0 . The remaining parameters are the normalized imposed field strength, $B_0/B_{\text{eq}0}$, turbulent viscosity and magnetic diffusivity, as well as the parameters q_{s0} and β_{σ} .

3 Results

3.1 Two- and three-dimensional solutions

Earlier work has suggested that the eigenmodes of NEMPI can be three-dimensional (BKR). This could render two-dimensional calculations inadequate if the first excited mode were indeed three-dimensional. However, it turns out that the wavelength of the eigenmode in the direction of the field increases as q_s decreases. In BKR, where three-dimensional (y -dependent) solutions to NEMPI were first reported, q_s was chosen to be around 10, and the fastest growing mode was indeed three-dimensional. In Fig. 1 we

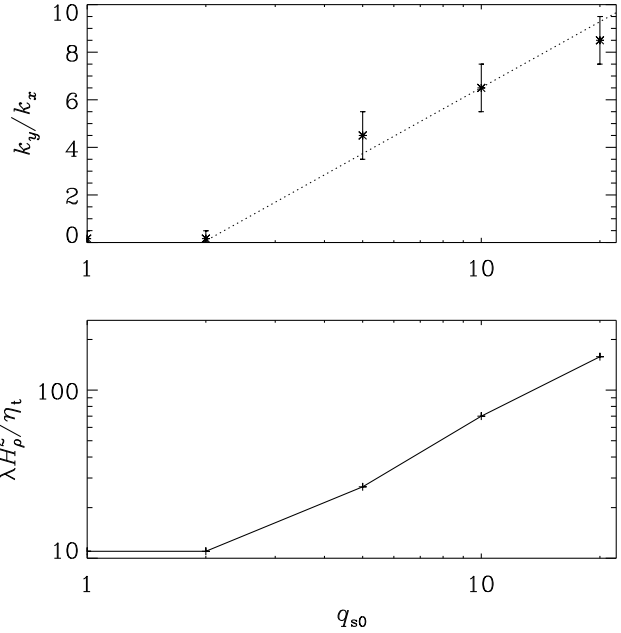


Fig. 2 Dependence of k_y on q_{s0} (upper panel), together with the corresponding growth rate λ (lower panel).

Table 1 Comparison of normalized growth rates, $\lambda H_{\rho}^2 / \eta_t$, for different values of q_s , for a three (3D) and two-dimensional (2D) simulation ($L_y \rightarrow \infty$).

$\lambda H_{\rho}^2 / \eta_t$	L_y / H_{ρ}	$q_s = 0$	$q_s = 20$
3D	2	11	158
2D	∞	11	11

show that the effective wavenumber of the variation of the field in the y direction decreases with decreasing values of q_s . This is shown quantitatively in Fig. 2, where we plot the dependence of the typical value of the field-aligned wavenumber, k_y , on the value of q_{s0} . Here, k_y is evaluated in a layer near the surface.

We find that the typical value of k_y grows with increasing values of q_{s0} . In addition, we find that the growth rate of the instability, λ , increases with q_{s0} approximately linearly once q_{s0} exceeds a value of around two. The fact that $k_y \rightarrow 0$ as $q_{s0} \rightarrow 0$ is significant, because BKKR and also Käpylä et al. (2012) found from simulations that $q_{s0} \approx 0$. In that case, the characteristic length scale along the direction of the field becomes infinite and the calculation essentially two-dimensional. Conversely, when studying NEMPI in two dimensions, changing the value of q_{s0} has no effect on structure formation and the growth rate; see Table 1. However, it is now clear that this is an artifact of restricting the solutions to be two-dimensional.

3.2 Approximate degeneracy in the q_p fit formula

We mentioned in the introduction that recent attempts to determine q_{p0} from simulations faced the difficulty that the fit

¹ <http://www.pencil-code.googlecode.com>

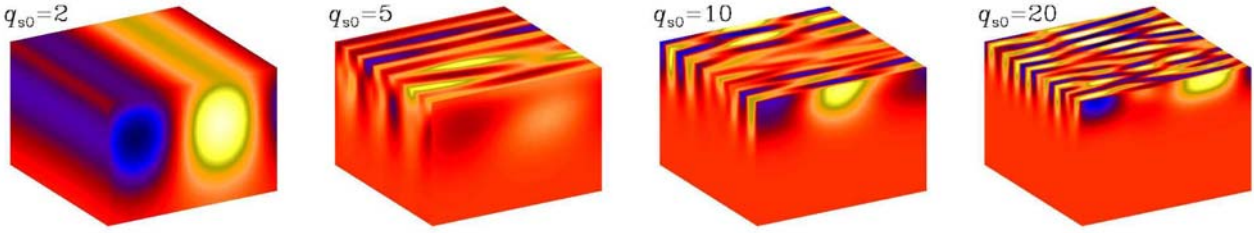


Fig. 1 (online colour at: www.an-journal.org) Visualization of \vec{B}_y at the periphery of the computational domain near the end of the kinematic growth phase. Note the change of the field pattern with increasing values of $q_{s0} = 2, 5, 10,$ and 20 (from left to right).

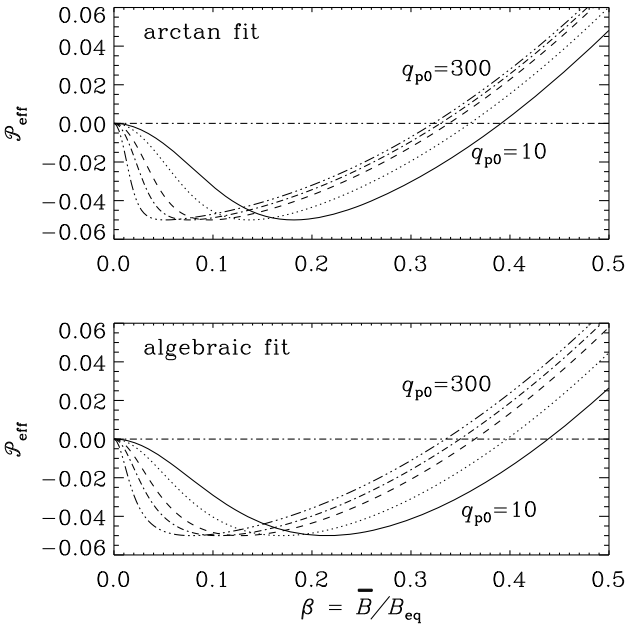


Fig. 3 *Top*: comparison of original fit curves with different q_{p0} values (10, 20, 50, 100, 300) and a fixed minimum, showing similar zero crossing values for a large q_{p0} range. *Bottom*: same as above, but now using an algebraic fit, giving larger spacing between the curves.

formula (7) possesses an approximate degeneracy in that we can obtain a similarly looking dependence of the effective mean magnetic pressure,

$$\mathcal{P}_{\text{eff}}(\beta) = \frac{1}{2}[1 - q_p(\beta)]\beta^2, \quad (11)$$

over a wide range of values of q_{p0} by adjusting the value of β_p correspondingly. This can be seen in Fig. 3, where we show $\mathcal{P}_{\text{eff}}(\beta)$ using either the arctan fit (upper panel) or the algebraic fit (lower panel) for parameters that result in the same value of \mathcal{P}_{min} for a range of values of q_{p0} . Note that the position where \mathcal{P}_{eff} becomes positive, i.e. the critical value defined by $\mathcal{P}_{\text{eff}}(\beta_{\text{crit}}) = 0$, is rather similar in all cases. This approximate degeneracy is particularly obvious for the arctan fit, and less so for the algebraic fit. However, in both cases the form of \mathcal{P}_{eff} near $\beta \rightarrow 0$ changes significantly. Therefore, the approximate degeneracy would be lifted if one could determine q_{p0} from the behavior of q_p near $\beta = 0$. However, near $\beta = 0$ the DNS have large errors.

It is therefore better to measure the normalized minimum effective magnetic pressure, $\mathcal{P}_{\text{min}} = \frac{1}{2} \min[(q_p - 1)\beta^2]$, and its position, β_{min} . For the algebraic fit we then obtain the fit parameters

$$\beta_p = \beta_{\text{min}}^2 / \sqrt{-2\mathcal{P}_{\text{min}}}, \quad \beta_* = \beta_p + \sqrt{-2\mathcal{P}_{\text{min}}}, \quad (12)$$

where we have introduced the parameter $\beta_*^2 = q_{p0}\beta_p^2$ in a modified representation

$$q_p(\beta) = \frac{\beta_*^2}{\beta_p^2 + \beta^2}, \quad (13)$$

which is preferable over Eq. (8) in circumstances where $\beta_*^2 = q_{p0}\beta_p^2$ is approximately constant. This appears to be the case in recent DNS (BKRR, Kemel et al. 2012), where $\beta_* \approx 0.2$ and 0.3 in the absence and presence of small-scale dynamo action, respectively.

We have computed mean-field models for different combinations of parameters using the algebraic fit. We find that the resulting growth rate λ depends on the functional form of $\mathcal{P}_{\text{eff}}(\beta)$ near $\beta = \beta_{\text{min}}$, which manifests itself in a dependence on both q_{p0} and β_p ; see Fig. 4. The lower panel of this figure suggests that the dependence of the growth rate on both parameters can be collapsed onto a single dependence on β_* . This underlines the usefulness of Eq. (13) as a fit formula. As argued above, this dependence is best constrained by the fit parameters β_{min} and \mathcal{P}_{min} .

3.3 Onset of NEMPI

With a given prescription of $q_p(\beta)$, assuming here $q_s = 0$, we can now compute two-dimensional mean-field models. Our goal is to obtain a simple formula that can tell us how large the growth rate of the instability is, and what the critical condition for the onset of the instability is. Not much is known about the linear stability properties of NEMPI, so we have to rely on numerical determinations of the growth rates for different wavelengths for different parameters to obtain an approximate representation of the dispersion relation. Earlier work of Kemel et al. (2011) has suggested a relation of the form

$$\lambda = \Phi(g/c_s^2, q_{p0}, \beta_p, \dots) - \nu_t k_\nu^2 - \eta_t k_\eta^2, \quad (14)$$

where k_ν and k_η are effective wavenumbers quantifying the effects of turbulent viscosity and turbulent magnetic diffusivity, Φ is a function of the inverse scale height, $H_\rho^{-1} =$

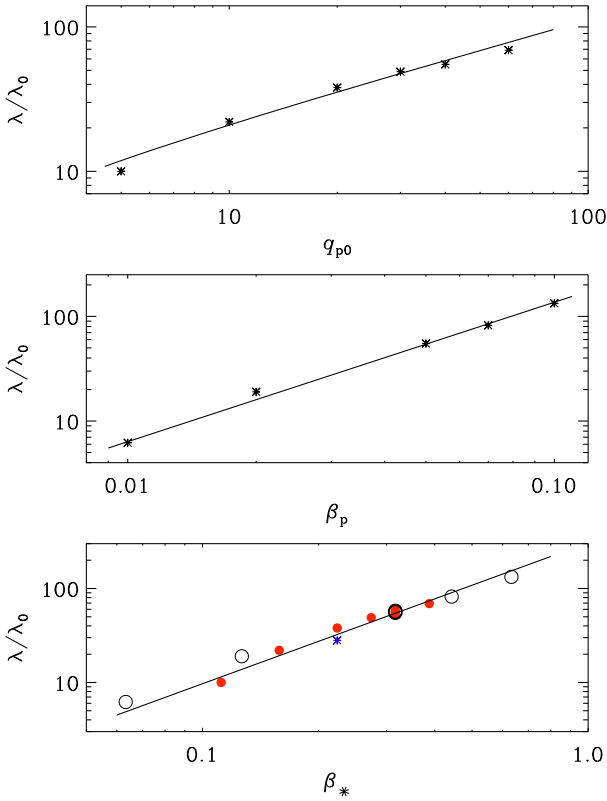


Fig. 4 Dependence of the normalized growth rate λ/λ_0 , with $\lambda_0 = (\nu_t + \eta_t)/H_\rho^2$, on q_{p0} for $\beta_p = 0.05$ (upper panel), on β_p for $q_{p0} = 40$ (middle panel), and on $\beta_* = q_{p0}^{1/2} \beta_p$ (lower panel) for $\beta_p = 0.05$ (red), $q_{p0} = 40$ (circles), and $\beta_p = 0.1$, $q_{p0} = 5$ (blue). Solid lines represent approximate fits given by $9(q_{p0} - 1)^{0.7}$, $(\beta_p/0.0015)^{1.3}$, and $(\beta_*/0.02)^{3/2}$, respectively.

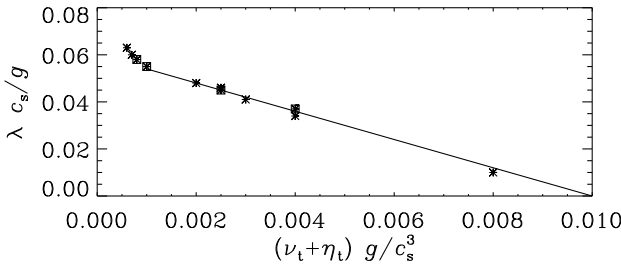


Fig. 5 Dependence of λ on $\nu_t + \eta_t$, normalized appropriately in terms of g and c_s . The negative slope gives k_d^2 with $k_d \approx 2.5/H_\rho$, where $H_\rho = c_s^2/g$.

g/c_s^2 , and other parameters describing the functional form of q_p .

We now need to determine the various unknowns. We begin by determining k_ν and k_η by varying either only ν_t or only η_t at a time. It turns out that $k_\nu = k_\eta \equiv k_d$ suffices. In this way we obtain a linear fit for the growth rate $\lambda = \text{const} - (\nu_t + \eta_t)k_d^2$, giving us k_d^2 as the slope of this graph; see Fig. 5. We find $k_d \approx 2.5/H_\rho$, superseding earlier results by Kemel et al. (2011) for a different $B_{\text{eq}}(z)$ profile.

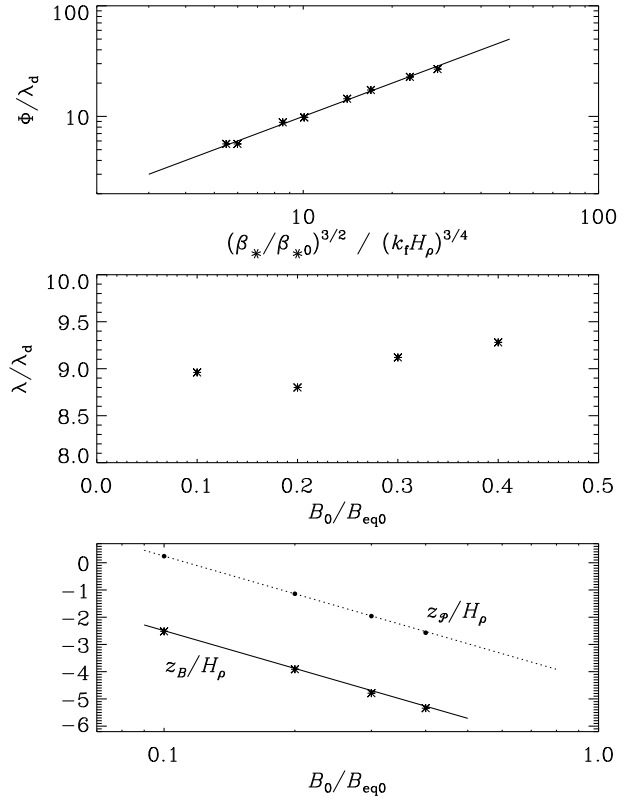


Fig. 6 Dependence of $\Phi = \lambda + (\nu_t + \eta_t)k_d^2$ on $(k_f H_\rho)^{-3/4}$ (upper panel), λ on $B_0/B_{\text{eq}0}$ (middle panel), as well as z_B/H_ρ and z_P/H_ρ on $B_0/B_{\text{eq}0}$ (lower panel). Here, $\beta_{*0} = 0.0083$ is a fit parameter and $\lambda_d = (\nu_t + \eta_t)k_d^2$ is used for normalization.

Accepting now the fit parameter k_d as measured, we can proceed to determining the dependence of Φ on H_ρ (top panel of Fig. 6). A convenient non-dimensional quantity is $k_f H_\rho$, where k_f is the wavenumber of the energy-carrying eddies of the turbulence, which is related to $\eta_t = u_{\text{rms}}/3k_f$ with $u_{\text{rms}} = B_{\text{eq}0}/\rho_0^{1/2}$. Note that $\Phi \propto (k_f H_\rho)^{-3/4}$. Combining this with the $\beta_*^{3/2}$ scaling of Fig. 4, we suggest

$$\lambda \approx \left[(\beta_*/\beta_{*0})^{3/2} (k_f H_\rho)^{-3/4} - 1 \right] (\nu_t + \eta_t)k_d^2, \quad (15)$$

with $\beta_{*0} \approx 0.008$ being yet another fit parameter. Interestingly, λ is independent of the imposed field strength, $B_0/B_{\text{eq}0}$, provided the bulk of the eigenmode ($z = z_B$) fits well within the domain (middle panel of Fig. 6). This has here been achieved by adjusting the positions of the boundaries, z_{top} and z_{bot} . Indeed, as $B_0/B_{\text{eq}0}$ is increased, z_B is found to decrease approximately like $z_B/H_\rho \approx -2 \ln B_0/B_{\text{eq}0} + \text{const}$. It turns out that z_B is about 2–3 scale heights below the location z_P where $\mathcal{P}_{\text{eff}}(z)$ attains its minimum value. Contrarily, when $z_P > z_{\text{bot}} > z_B$ or when $z_{\text{top}} < z_B$ NEMPI will depend on respectively β_{bot} or β_{top} , when $z_P < z_{\text{bot}}$ there is no instability.

Some comments about the horizontal dimensions are in order. In all cases with $q_{s0} = 0$, we find that in three-dimensional calculations with finite y extent, the value of L_y does not affect the growth rates. On the other hand, dou-

bling the x extent yields two pairs of rolls. This has also been confirmed for DNS; see Kemel et al. (2012).

4 Conclusions

The present work has clarified a number of puzzling aspects of NEMPI. Firstly, it is now clear that we can proceed with two-dimensional mean-field simulations as long as we know that $q_{s0} = 0$ (or negative). However, this may not always be the case. The fact that three-dimensional structures can emerge from NEMPI was initially thought to be an interesting aspect, because it could readily explain the formation of bipolar regions (BKR). However, given that simulations now indicate that $q_s \approx 0$ (or perhaps even negative), this proposal would thus not be an option, unless some other as yet unexplored effect begins to play a role. In principle, all turbulent transport processes are nonlocal and must be described by a convolution with the mean field rather than a multiplication (Brandenburg et al. 2008). In Fourier space, the convolution corresponds to a multiplication with a wavenumber-dependent turbulent transport coefficient. Thus, the idea of explaining bipolar regions would again become viable if this effect only existed at small and intermediate length scales. Clarifying this would be a task for future simulations, because none of the currently available techniques are yet equipped to address this possibility.

Next, we have seen that the degeneracy in the fit formula used for $q_p(\beta)$ and $\mathcal{P}_{\text{eff}}(\beta)$ is significant in that different combinations of q_{p0} and β_p result in similar values of $\min(\mathcal{P}_{\text{eff}})$ and β_{crit} , but the growth rates can still be quite different. This means that it is not sufficient to measure only $\min(\mathcal{P}_{\text{eff}})$ and β_{crit} . Instead, to characterize the functional form of $\mathcal{P}_{\text{eff}}(\beta)$ more accurately, we need some other characteristics to represent the dependence of this function near $\beta = 0$. One such possibility is to use the field strength β_{min} for which the minimum of the effective magnetic pressure is reached.

Knowing the value of β_{min} has particular relevance in determining the height where NEMPI occurs. For a given value of the imposed field strength B_0 , the condition $B_0/B_{\text{eq}}(z_{\mathcal{P}}) = \beta_{\text{min}}$ determines the height $z_{\mathcal{P}}$, where the effective magnetic pressure attains a minimum, and thus the height z_B , which tends to be 2–3 scale heights below z_{min} ; see the lower panel of Fig. 6. Therefore, the value of B_0 does not directly affect the growth rate of NEMPI.

Finally, we have tried to establish an approximate dispersion relation to estimate the growth rate of NEMPI as a function of turbulent viscosity, turbulent magnetic diffusivity, mean field strength, and the strength of stratification. This formula may serve as a first orientation and can hopefully be improved further with future simulations. This formula can also be useful in connection with analytic estimates concerning the regimes when NEMPI is expected in DNS or under other more realistic circumstances.

Acknowledgements. We thank the anonymous reviewer for making useful suggestions. We acknowledge the NORDITA dynamo

programs of 2009 and 2011 for providing a stimulating scientific atmosphere. Computing resources provided by the Swedish National Allocations Committee at the Center for Parallel Computers at the Royal Institute of Technology in Stockholm, the National Supercomputing Center in Linköping, and the High Performance Computing Center North in Umeå. This work was supported in part by the European Research Council under the AstroDyn project 227952 and the Swedish Research Council grant 621-2011-5076.

References

- Brandenburg, A., von Rekowski, B.: 2001, *A&A* 379, 1153
 Brandenburg, A., Kleeorin, N., Rogachevskii, I.: 2010, *AN* 331, 5 (BKR)
 Brandenburg, A., Kemel, K., Kleeorin, N., Mitra, D., Rogachevskii, I.: 2011, *ApJ* 740, L50 (BKKMR)
 Brandenburg, A., Kemel, K., Kleeorin, N., Rogachevskii, I.: 2012, *ApJ*, submitted, astro-ph/1005.5700 (BKKR)
 Brandenburg, A., Rädler, K.-H., Schrunner, M.: 2008, *A&A* 482, 739
 Courvoisier, A., Hughes, D.W., Proctor, M.R.E.: 2010, *Proc. Roy. Soc. Lond.* 466, 583
 Frisch, U., She, Z.S., Sulem, P.L.: 1987, *Physica* 28D, 382
 Käpylä, P.J., Brandenburg, A., Kleeorin, N., Mantere, M.J., Rogachevskii, I.: 2012, *MNRAS*, submitted, astro-ph/1104.4541
 Kemel, K., Brandenburg, A., Kleeorin, N., Rogachevskii, I.: 2011, in: A. Bonanno, E. de Gouveia dal Pino, A. Kosovichev (eds.), *Advances in Plasma Astrophysics*, IAU Symp. 274, p.473
 Kemel, K., Brandenburg, A., Kleeorin, N., Mitra, D., & Rogachevskii, I.: 2012, *Sol. Phys.*, submitted, astro-ph/1112.0279
 Kitiashvili, I.N., Kosovichev, A.G., Wray, A.A., Mansour, N.N.: 2010, *ApJ* 719, 307
 Kleeorin, N., Rogachevskii, I.: 1994, *Phys. Rev. E* 50, 2716
 Kleeorin, N., Mond, M., Rogachevskii, I.: 1993, *Phys. Fluids B*, 5, 4128
 Kleeorin, N., Mond, M., Rogachevskii, I.: 1996, *A&A* 307, 293
 Kleeorin, N.I., Rogachevskii, I.V., Ruzmaikin, A.A.: 1989, *Sov. Astron. Lett.* 15, 274
 Kleeorin, N.I., Rogachevskii, I.V., Ruzmaikin, A.A.: 1990, *Sov. Phys. JETP* 70, 878
 Newcomb, W.A.: 1961, *Phys. Fluids* 4, 391
 Parker, E.N.: 1966, *ApJ* 145, 811
 Priest, E.R.: 1982, *Solar Magnetohydrodynamics*, D. Reidel Publ. Co., Dordrecht
 Rädler, K.-H.: 1974, *AN* 295, 265
 Roberts, P.H., Soward, A.M.: 1975, *AN* 296, 49
 Rogachevskii, I., Kleeorin, N.: 2007, *Phys. Rev. E* 76, 056307
 Rüdiger, G.: 1974, *AN* 295, 275
 Rüdiger, G.: 1980, *Geophys. Astrophys. Fluid Dyn.* 16, 239
 Rüdiger, G.: 1989, *Differential Rotation and Stellar Convection: Sun and Solar-Type Stars*, Gordon & Breach, New York
 Rüdiger, G., Hollerbach, R.: 2004, *The Magnetic Universe: Geophysical and Astrophysical Dynamo Theory*, Wiley-VCH, Berlin
 Rüdiger, G., Tuominen, I., Krause, F., Virtanen, H.: 1986, *A&A* 166, 306
 Rüdiger, G., Kitchatinov, L.L., Schultz, M.: 2012, *AN* 333, 84
 Tao, L., Weiss, N.O., Brownjohn, D.P., Proctor, M.R.E.: 1998, *ApJ* 496, L39
 Tserkovnikov, Y.A.: 1960, *Sov. Phys. Dokl.* 5, 87